

Received June 9, 2014; reviewed; accepted September 21, 2014

RECOVERY MECHANISMS OF SERICITE IN MICROCRYSTALLINE GRAPHITE FLOTATION

Hongqiang LI^{*}, Leming OU^{**}, Qiming FENG^{**}, Ziyong CHANG^{**}

^{*} College of Resource and Environmental Engineering, Wuhan University of Technology, Wuhan 430070, PR China

^{**} School of Mineral Processing and Bioengineering, Central South University, Changsha 410083, PR China, olm@mail.csu.edu.cn

Abstract: Sericite is the main contaminant of concentrate in commercial microcrystalline graphite ore flotation. It was necessary to identify its recovery mechanisms so that the appropriate solution can be selected. In this study, the influence of sericite on flotation selectivity of microcrystalline graphite ore and its recovery mechanisms were investigated. Artificial mixtures flotation test suggested that sericite seriously reported into concentrate leading to poor flotation selectivity of microcrystalline graphite ore. However, the aggregation/dispersion behavior of artificial mixtures indicated that a large repulsive energy existed between sericite and microcrystalline graphite particles at pH 7.4, and sericite was not likely to report into graphite concentrate by slime coating. The results obtained from contact angle measurements and a technique of Warren showed that the floated sericite reached the froth via a combination of both entrainment and entrapment mechanisms, not via true flotation.

Keywords: *microcrystalline graphite, sericite, flotation, entrainment, entrapment*

Introduction

Natural graphite forms from the metamorphism of organic carbon or carbonaceous rocks and is found in three commercial varieties: crystalline flake, microcrystalline, and crystalline vein (Crossley, 1999). Some microcrystalline graphite deposits usually have a high air dried basis fixed carbon content (FC_{ad}) ($FC_{ad} > 80$ wt.%), and can be marketed after selective mining and a minimum processing. However, the average FC_{ad} of some European deposits is as low as 55 wt.% (Simandl and Kenanl, 1997) while in China the FC_{ad} of some microcrystalline graphite deposits is 50-70 wt.%. So far, a number of research projects have been undertaken to purify those low-grade microcrystalline graphite ores, flotation and chemical purification are commonly used. Chemical purification is an effective beneficiation method, including alkali roasting,

hydrofluoric acid treatment and chlorination roasting, but it easily leads to environment pollution while flotation is a low cost and environment friendly method compared with chemical purification (Dong, 1997).

For commercial microcrystalline graphite ore with FC_{ad} of 60-70wt.%, it can only be upgraded to 80-88wt.% (FC_{ad}) by flotation (Ji, 1991; Xia et al., 1996; Dong, 1997), and the primary contaminant of concentrate is sericite, which is a fine grained muscovite mica. Sericite also occurs in many base metal ore bodies, and it is often recovered strongly into the final flotation concentrate (Silvester, 2011). It has been hypothesized that liberated sericite may be collected in the froth product by true flotation due to surface hydrophobicity (Blaskett, 1960) or slime coating (He, 2009). A wide range of sericite depressants or dispersants has been tried over the years, but it does not appear to respond readily to those conventional reagents, and mostly ends up as a significant diluent in the final concentrate, which suggests that the mechanism of sericite recovery is not properly understood. Before the best mean for preventing liberated sericite recovery can be selected, it is necessary to determine how the sericite is actually being recovered.

In this study, in order to simulate the flotation process of microcrystalline graphite ore, batch flotation test of artificial mixtures in -30 μm size fraction was carried out. To demonstrate how sericite particles were reaching the froth phase, and determine which class of sericite particles (floating particles due to hydrophobicity, hetero-coagulation particles or entrained particles) was the most important contributor to sericite recovery in froth flotation, contact angle measurements, zeta potential measurements, and a technique of assessment of true flotation and entrainment of mineral have been applied (George et al., 2004).

Materials and methods

Materials

The sericite used for all experiments was obtained from Xiangyang, Hubei Province, China. The sample was dry ground and screened, and the -97 μm size fraction was collected and used in the experiments. X-ray fluorescence (XRF) analysis indicated that it contains 8.877 wt.% K_2O , 0.69 wt.% Na_2O , 36.59 wt.% Al_2O_3 , and 47.11 wt.% SiO_2 . The software Jade 5.0 was used to analysis X-ray diffraction pattern. Figure 1(a) is the X-ray diffraction pattern of sericite, which indicated that the purity of the sericite is 92 wt.%.

The microcrystalline graphite was obtained from the Hunan Lutang Graphite Mine located in the Beihu district of the Chenzhou city. It was processed using the same method as sericite. The results of proximate analysis (volatile matter, fixed carbon, and ash) of microcrystalline graphite revealed that the air dried basis volatile matter (V_{ad}) was 3.25 wt.%, the air dried basis ash content (A_{ad}) was 6.63wt.%, and the FC_{ad} was 90.12 wt.%. Figure 1(b) shows the X-ray diffraction pattern of the microcrystalline graphite sample. Based on the results of proximate analysis and X-ray

diffraction, it can be concluded that the purity of graphite sample obtained was 93 wt.%.

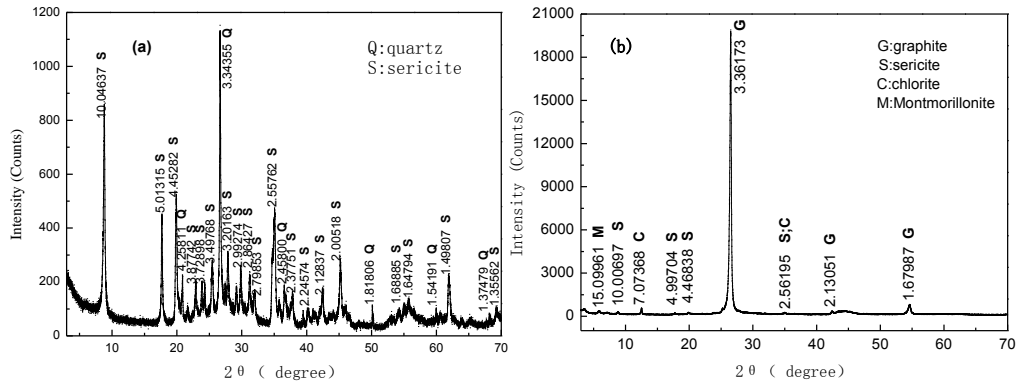


Fig. 1. XRD patterns of single minerals (a) sericite (b) microcrystalline graphite

Particle size distributions of test samples were determined by a Mastersizer 2000 particle size analyzer, and the results are seen in Table 1 and Fig. 2. kerosene used as a collector was emulsified in a high-speed blender at a concentration of 1 g/dm³. The median size of the kerosene droplets emulsified with addition of surfactants was below 4 μm and the droplet size was also determined by Mastersizer 2000 particle size analyzer. Additionally, methyl isobutyl carbinol (MIBC) was used as a frother.

Table 1. Particle size distribution of single minerals

Single mineral	D_{10} (μm)	D_{50} (μm)	D_{90} (μm)	Average diameter (μm)
Microcrystalline graphite (-97 μm)	2.729	34.375	90.207	46.736
Sericite (-97 μm)	2.016	20.379	76.296	30.739

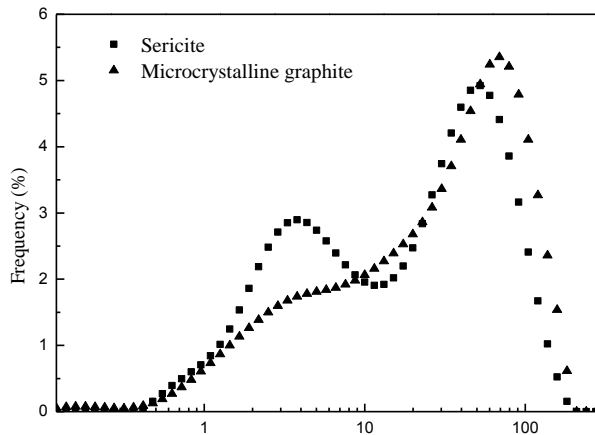


Fig. 2. Particle size distribution of single minerals

Methods

Contact angle measurements

These experiments were implemented to determine the hydrophobicity of sericite at different kerosene dosages. The assessments of hydrophobicity of sericite powder were carried out on GBX MiniLab ILMS using the Washburn technique (Chibowski and Perea-Carpio, 2002). The flotation tests were conducted in water, thus the reference liquid was water. The results were checked by the sessile drop on polished surface of sericite block. The data were the average value of five separate determinations. The experimental error of the contact angle measurements was within $\pm 10\%$.

Batch flotation tests of artificial mixtures of microcrystalline graphite–sericite

These tests were carried out to assess the influence of sericite recovery on flotation selectivity of microcrystalline graphite. Based on the vast difference of floatability between hydrophobic graphite and hydrophilic sericite, the recovery of sericite was determined when all of the microcrystalline graphite was recovered into the concentrate. The tests were conducted in an XFD-type laboratory flotation machine (1 dm^3), and the flotation experimental error was within $\pm 5\%$. The artificial mixtures slurry was composed of 2.5wt.% sericite and 15 wt.% graphite. Both sericite and microcrystalline graphite were in the same size fraction ($-30 \mu\text{m}$).

Firstly, the original weight of tap water (W_0) was recorded, the slurry in flotation cell was prepared by adding artificial mixtures of microcrystalline graphite (W_g)–sericite (W_s) to tap water followed by adding the collector kerosene (1.3 kg/Mg) and frother MIBC (100 g/Mg) to the slurry. Then, the flotation froth was scraped into the plastic basin every 10 s for 12 min, all of the graphite was scraped out at this point, the froth depth was controlled at about 20 mm through adding tap water, and the plastic basin with concentrate (W_{c1}), and tap water left (W_1) should be weighed. Finally, the tailing left in flotation cell was collected and filtrated, the filtrated tailing and the plastic basin with concentrate were dried at $80 \text{ }^\circ\text{C}$ in an oven, weighed and recorded as (W_t) and (W_{c2}). The recovery of water and sericite can be calculated by Eqs. 1 and 2

$$R_w = \frac{W_{c1} - W_{c2}}{W_0 - W_1} \cdot 100\% \quad (1)$$

where

R_w – recovery of water (%)

W_0 – original weight of tap water (g)

W_1 – weight of tap water left (g)

W_{c1} – wet weight of plastic basin with concentrate (g)

W_{c2} – dry weight of plastic basin with concentrate (g)

$$R_s = \left(1 - \frac{W_t}{W_s} \right) \cdot 100\% \quad (2)$$

R_s – recovery of sericite in graphite concentrate (%)

W_t – dry weight of tailing (g)

W_s – dry weight of sericite in feed (g).

Zeta potential measurements

The zeta potential measurements were performed using a ZetaPALS zeta potential analyzer, the experimental error of zeta potential measurement was within $\pm 10\%$. To prepare the stock suspension, 1 g of the mineral ($- 4 \mu\text{m}$) was added to a 1 dm^3 volumetric flask containing $10^{-2} \text{ mol/dm}^3 \text{ KNO}_3$ solution. For each zeta potential measurement, 10 cm^3 of the stock mineral slurry was withdrawn and diluted with 90 cm^3 of $10^{-2} \text{ mol/dm}^3 \text{ KNO}_3$ solution, adjusted to appropriate pH using NaOH or HCl, and then treated by desired reagents. A very small amount (about 2 cm^3) of this conditioned particle slurry was transferred to the plastic sample cell of the ZetaPALS for zeta potential measurement. The zeta potential measurement was carried out from low pH upwards, when a test was finished, another 10 cm^3 of the stock mineral slurry was withdrawn for zeta potential of a higher pH.

Assessment of true flotation and entrainment of sericite

These tests were used for determination of true flotation and entrainment of sericite in the presence of microcrystalline graphite. This technique, proposed by Warren, assumes that particle entrainment does not take place in a dry froth (Warren 1985). A series of experiments were conducted, and the rate of water recovery was varied by changing the rate of froth removal or froth depth. A regression line for the relationship between total solids recovery and water recovery was extrapolated to a zero water recovery. The mass of solids recovered at this point is the recovery by true flotation alone. This technique could be summarized as seen in Eq. 3:

$$R_m(t) = F + R_E = F + e \times R_w(t) \quad (3)$$

$R_m(t)$ – total recovery of solids by true flotation and entrainment (%)

F – recovery of solids due to true flotation (%)

R_E – recovery of solids due to entrainment (%)

$R_w(t)$ – recovery of water (%)

e – degree of entrainment

where, e is equal to the slope of $R_m(t)$ versus $R_w(t)$. A schematic representation of this technique is shown in Fig. 3.

The tests were conducted, and the rate of water recovery was varied by changing froth depth as 10 mm, 20 mm, and 30 mm, and the J_g was fixed at $3.3 \text{ dm}^3/\text{min}$ for each test. The artificial mixtures slurry was composed of 6.6 wt.% sericite and 13.4 wt.% graphite. The dosages of kerosene and MIBC were chosen as 1300 g/Mg and

100 g/Mg, respectively. The impeller speed was kept constant at 1080 rpm. Time $t=0$ was taken as the instant the froth overflowed into the first froth collecting tray, the froth was removed at a constant, controlled rate of 6 scrapes per minute. Timed samples were obtained at cumulative flotation times of 0.5, 1, 1.5, 2, 3, 4, and 8 min, and the flotation experimental error was within $\pm 5\%$.

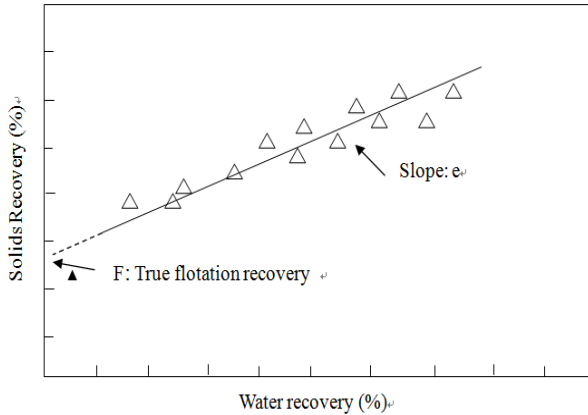


Fig. 3. Determination of true flotation by the Warren method

Theoretical background

Hetero-coagulation, which leads to slime coating between valuable mineral and gangue, is usually described by the DLVO theory (Adamczyk, 1999), the colloidal forces considered include the electrostatic double-layer force and the Van der Waals force.

Electrostatic double-layer (EDL) interaction

The model used to describe the Electrostatic Double-Layer (EDL) interaction energy is based on the Poisson–Boltzmann equation, which describes the electrostatic potential in an ionic solution as a function of position relative to the particle surface, and has been found to be accurate down to separations of a few nanometers (Mitchell et al., 2005). The interaction energy at constant surface potentials is often used, and can be described by Eq. 4:

$$V_E = \frac{\pi\epsilon_0\epsilon_r R_1 R_2}{(R_1 + R_2)} (\psi_1^2 + \psi_2^2) \cdot \left\{ \frac{2\psi_1\psi_2}{(\psi_1^2 + \psi_2^2)} \cdot \ln \left[\frac{1 + \exp(-\kappa H)}{1 - \exp(-\kappa H)} \right] + \ln [1 - \exp(-2\kappa H)] \right\} \quad (4)$$

where the average radius of sericite particle R_1 was 15.37 μm (Table 1), the average radius of microcrystalline graphite particle R_2 was 23.37 μm (Table 1); $1/\kappa$ is the electrical double layer thickness in which $\kappa = 0.10 \text{ nm}^{-1}$ (Wan, 1997); ϵ_0, ϵ_r represent the vacuum dielectric constant and the relative dielectric constant of continuous phase, respectively. The given value of $\epsilon_0 \cdot \epsilon_r$ was $6.95 \cdot 10^{-10} \text{ C}^2 \cdot (\text{J} \cdot \text{m})^{-1}$, H represents the

distance between particles, ψ_1 and ψ_2 are the surface potential. When contact time between the particles is very short, the assumption of constant surface charge is appropriate (Nguyen, 2002).

Van der Waals interaction

The Van der Waals interaction energy is calculated using Eq. 5:

$$V_w = -\frac{A}{6H} \cdot \frac{R_1 R_2}{(R_1 + R_2)} \quad (5)$$

The Hamaker constant (A) for sericite/water/graphite is not available in literature. For mica, the value of the Hamaker constant acting through vacuum was $9.86 \cdot 10^{-20}$ J (Bergstrom 1997). Sericite is fine grained mica, thus the Hamaker constant of sericite (A_{11}) could be chosen as $9.86 \cdot 10^{-20}$ J. The Hamaker constant of graphite in vacuum is $23.8 \cdot 10^{-20}$ J (Maurer et al., 2001), because microcrystalline graphite is fine grain graphite, the Hamaker Constant of microcrystalline graphite (A_{22}) could be chosen as $23.8 \cdot 10^{-20}$ J. The Hamaker constant (A_{123}) for two different materials (1 and 2) interacting through medium 3 is (Eq. 6):

$$A_{132} = (\sqrt{A_{11}} - \sqrt{A_{33}})(\sqrt{A_{22}} - \sqrt{A_{33}}) \quad (6)$$

When medium 3 is water ($A_{33} = 3.7 \times 10^{-20}$ J), a value of the Hamaker constant of $4.45 \cdot 10^{-20}$ J was calculated for the sericite/ water/ microcrystalline graphite system on the basis of Eq. 6, and this value was used in this study.

Results and discussion

Influence of sericite recovery on flotation selectivity of microcrystalline graphite ore

During the multistage cleaning processes of commercial microcrystalline graphite ore, the enrichment ratio (E_r) decreased sharply, especially when the FC_{ad} of feed was above 85 wt.%, it was difficult to upgrade further by flotation. This was illustrated in previous literature clearly (Li, 2014). To simulate flotation process of commercial microcrystalline graphite ore, artificial mixtures with the same FC_{ad} (85 wt.%) should be selected.

For the purpose of assess the effect of sericite recovery on the enrichment ratio in artificial mixtures flotation and it was supposed that FC_{ad} of microcrystalline graphite single mineral was 100 wt.%, the equivalent FC_{ad} (FC_{ad}^*) of artificial mixtures feed could be calculated by Eq. 7:

$$FC_{ad}^* = \frac{C_g}{C_g + C_s} \cdot 100\% \quad (7)$$

FC_{ad}^* – equivalent FC_{ad} of artificial mixtures, ignoring the ash and volatile of graphite, wt. %

C_g – sub-concentrate of microcrystalline graphite in slurry, wt. %

C_s – sub-concentrate of sericite in slurry, wt. %.

In this section, artificial mixtures ($FC_{ad}^*=85.72$ wt.%) was selected. The artificial mixtures slurry was composed of 2.5 wt.% sericite and 15 wt.% graphite.

E_r could be calculated with Eq. 8, $(100-FC_{ad}^*)$ was the content of sericite in feed, $(100-R_s)$ represented the amount of sericite that was rejected as tailing:

$$E_r = \frac{\beta}{\alpha} = \frac{FC_{ad}^* + (100 - FC_{ad}^*)(100 - R_s) / 100}{FC_{ad}^*} = 1 + \frac{(100 - FC_{ad}^*)(100 - R_s)}{100 \cdot FC_{ad}^*} \quad (8)$$

β – grade of concentrate, wt. %

α – grade of feed, wt. %

FC_{ad}^* – equivalent FC_{ad} of feed, wt. %

E_r – enrichment ratio

R_s – recovery of sericite, %.

The commercial microcrystalline graphite ore was usually ground to more than 90% or even 100% pass through -30 μm sieve to liberate graphite from gangue minerals, thus, artificial mixtures in -30 μm size fraction was selected.

The FC_{ad}^* of feed after one stage flotation was 85.70%. FC_{ad}^* of the concentrate was only 87.5% due to 88.02% of sericite recovered in graphite concentrate, and the enrichment ratio was only 1.02. These results suggested that the serious misreport of sericite led to poor flotation selectivity when microcrystalline graphite ore was fine ground.

There are several mechanisms which have been proposed by which liberated gangue particles may be collected in the concentrate:

- via true flotation if the conditioning step applied makes the minerals hydrophobic,
- via aggregation with the valuable mineral,
- via entrainment or entrapment.

In order to determine mechanisms by which liberated sericite may be collected into the concentrate in artificial mixtures flotation, three sets of experiments were carried out.

Effect of kerosene dosage on wettability of sericite

Kerosene is widely used as a collector in graphite flotation (Salgado, 2001). In order to assess the effect of kerosene dosage on the hydrophobicity of sericite, the contact angle of sericite powder at different kerosene dosages was measured. The results are presented in Table 2.

It can be seen from Table 2 that the contact angle of sericite powder was 16.78° in the absence of kerosene, indicating that sericite was almost a hydrophilic mineral,

which was in agreement with earlier observation (Gao et al., 2007). As the kerosene dosage increased from 0 to 2000 g/Mg, the average contact angle of sericite powder was not changed. The result indicated that kerosene did not improve the surface hydrophobicity of sericite, and sericite would not report into concentrate by true flotation when kerosene was used as the collector.

Table 2. Contact angle of sericite powder at different kerosene dosages

Kerosene dosage (g/Mg)	Contact angle (°)
0	16.78
250	17.20
500	16.55
750	16.05
1000	17.09
1500	16.85
2000	17.05

Aggregation/dispersion behaviors of microcrystalline graphite and sericite particles

The aggregation/dispersion behaviors of gangue mineral and valuable mineral particles were usually evaluated from particle interaction energy, particle interaction energy in aqueous solution is commonly described through application of DLVO theory, which allows quantitative prediction of the interaction energy. If particle interaction energy was negative, hetero-coagulation (slime coating) was unavoidable.

The zeta potential values of the sericite and microcrystalline graphite are shown in Figs. 4(a) and (b), respectively.

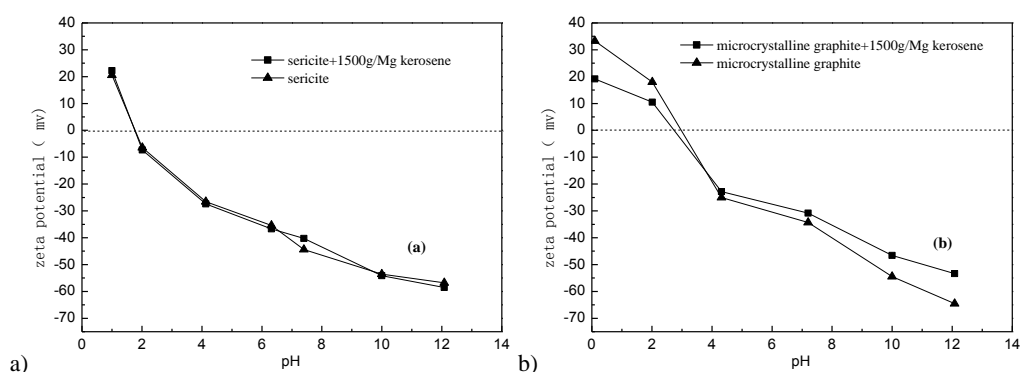


Fig. 4. Zeta potential of (a) sericite (b) microcrystalline graphite as a function of pH in the absence and presence of kerosene

In the absence of kerosene, the zeta potential value of sericite at pH 7.4 was -44.38 mV, and that of the microcrystalline graphite was -34.32 mV. When kerosene dosage

was 1300 g/Mg, the zeta potential of sericite was -45.45 mV, that is almost the same as that of original sericite. The results indicated that kerosene did not adsorb on sericite surface, which agreed with the results of the contact angle measurements. Different from sericite, when kerosene dosage was 1300 g/Mg, the zeta potential of microcrystalline graphite changed to -30.83 mV from -34.32 mV. The absolute value of the zeta potential of microcrystalline graphite decreased in the pH value range of 0-12 because of the adsorption of kerosene on the mineral surface.

The total interaction energy V_T^D was calculated by replacing the relative data using Eqs. 4 and 5, and the results are shown in Fig. 5. The maximum value of total interaction energy V_T^D was 38.07×10^{-18} J when the particle distance was 4.24 nm indicating that sericite and microcrystalline graphite particles must overcome this large repulsive energy to form aggregates. It is suggested that aggregates between sericite and microcrystalline graphite particles did not form during artificial mixtures flotation, sericite was not likely to report into graphite concentrate by slime coating (sericite-microcrystalline graphite aggregates).

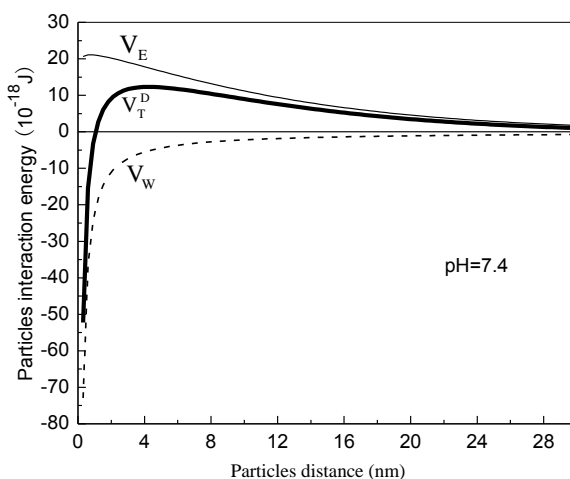


Fig. 5. Interaction energy between sericite and microcrystalline graphite particles in the presence of 1300 g/Mg kerosene at pH=7.4

Determination of true flotation and entrainment of sericite

To evaluate the quantity of sericite recovered by true flotation and entrainment in flotation of microcrystalline graphite, the technique proposed by Warren (1985) was applied.

The interval entrainment factor $e(t)$ and cumulative entrainment factor $e^c(t)$ in a given time could be calculated by Eqs. 9 and 10, respectively:

$$e(t) = \frac{R_s(t)}{R_w(t)} \quad (9)$$

$R_s(t)$ – recovery of sericite in a given time (%)

$R_w(t)$ – recovery of water in a given time (%)

$e(t)$ – interval entrainment factor in a given time

$$e^c(t) = \frac{R_s^c(t)}{R_w^c(t)} \quad (10)$$

$R_{sc}^c(t)$ – cumulative recovery of sericite in a given time (%)

$R_w^c(t)$ – cumulative recovery of water in a given time (%)

$e^c(t)$ – cumulative entrainment factor in a given time.

Table 3. Correlation (e) between solid recovery and water recovery during the batch flotation tests

Froth depth (mm)	Time interval (min)	$R_w^c(t)$ (%)	$R_s^c(t)$ (%)	$e(t)$	$e^c(t)$
10	0~0.5	9.32	10.29	1.10	1.10
	0.5~1.0	20.30	20.12	0.90	0.99
	1~1.5	27.87	25.23	0.67	0.91
	1.5~2	32.85	29.31	0.82	0.89
	2~3	36.44	29.77	0.13	0.82
	3~4	38.31	30.31	0.29	0.79
	4~8	40.70	30.79	0.20	0.76
20	0~0.5	4.31	5.07	1.18	1.18
	0.5~1.0	10.59	12.49	1.18	1.18
	1~1.5	15.83	17.23	0.90	1.09
	1.5~2	21.06	20.84	0.69	0.99
	2~3	27.86	24.16	0.49	0.87
	3~4	35.28	24.97	0.11	0.71
	4~8	41.03	26.49	0.26	0.65
30	0~0.5	7.38	9.52	1.29	1.29
	0.5~1.0	12.97	16.12	1.18	1.24
	1~1.5	19.86	22.53	0.93	1.13
	1.5~2	27.04	27.11	0.64	1.00
	2~3	33.99	29.82	0.39	0.88
	3~4	40.13	31.51	0.28	0.79
	4~8	43.75	31.93	0.12	0.73

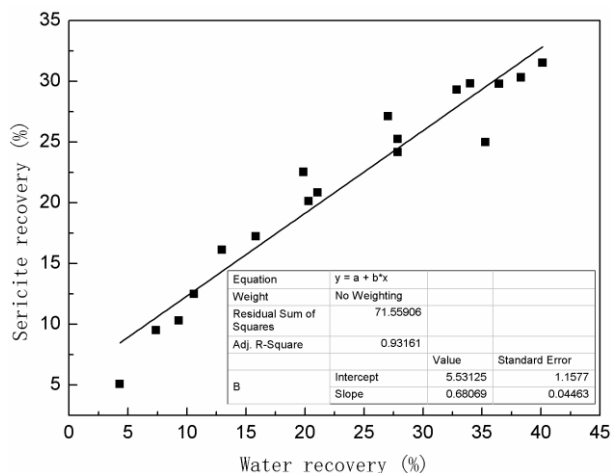


Fig. 6. Recovery of sericite versus water recovery obtained using the technique of Warren

Warren (1985) found that the correlation (entrainment factor) between solid recovery and water recovery normally deteriorated with time. As shown in Table 3, e of sericite decreased with the increase of the flotation time. When the froth depth was 30 mm, e of sericite was 1.29 over the first 0.5 min and it decreased to 0.12 over the last 4 min. Therefore, this method should ideally be applied over a flotation time that is just long enough for the recovery of most, but not all, of the easily floatable solids. In this section, the proper time interval was chosen between 0 and 4 min.

A plot of the recovery of sericite versus water recovery is seen in Fig. 6. The procedure of Warren assumes that entrainment occurs when particles are transported in the interstitial liquid. When the line of best fit was extrapolated to zero water recovery, the intercept was about 5.5%, the overall recovery of sericite was about 32%, indicating that around 17% of all recovered sericite was captured by true flotation, and about 83% of all floated sericite was recovered by entrainment. However, as the kerosene dosage increased from 0 to 2000 g/Mg, the average contact angle of sericite powder ranged from 16.05° to 17.20° and it was impossible for sericite to be recovered by true flotation. In all of the tests, $e(t)$ of sericite was greater than one over the first 0.5 min, as shown in Table 3, similar results was found in literature of (Wang and Peng, 2013). Zheng et al. (2006) claimed that if the entrapment was an additional mechanism for the recovery of liberated silica particles, it was possible in practice for the calculated entrainment factor (e) value to be greater than 1. It is suggested that entrapment may be an additional mechanism for sericite recovery.

In well-drained froths, entrained particles and water drain from the froth rapidly near the pulp-froth interface, but the entrained particles become entrapped between the bubble films at increased heights in the froth. It is therefore reasonable to postulate that as the bubble films grow thinner with increasing height in the froth (as a result of drainage), the probability of entrained particles becoming trapped in these films will

increase. Over the first 0.5 min, e of sericite was 1.10 when the froth depth was 10 mm, e of sericite increased to 1.29 with the increasing of the froth depth to 30 mm. It was shown that the quantity of sericite reporting to concentrate by entrapment increased with the increase of the froth depth.

The results obtained by the technique of Warren and the contact angle measurements showed that while the majority of sericite was recovered into the concentrate as a result of entrainment, part of sericite was recovered into the concentrate by entrapment, and no sericite was recovered via true flotation.

Conclusions

In this study, the recovery mechanisms of sericite and their effect on microcrystalline graphite flotation were investigated. The following conclusions were drawn from the above observations.

The batch flotation tests of artificial mixtures indicated that the poor flotation selectivity of commercial microcrystalline graphite ore was attributed to the serious misreport of sericite into concentrate.

The aggregation/dispersion behaviors of microcrystalline graphite and sericite particles suggested that sericite was not likely to report into graphite concentrate by slime coating.

Sericite was a hydrophilic mineral, and kerosene did not change its surface hydrophobicity therefore it was impossible for sericite to be recovered by true flotation in microcrystalline graphite flotation.

From the results obtained by the technique of Warren and the contact angle measurements it can be concluded that the majority of sericite was recovered into the concentrate as a result of entrainment and a part of sericite was recovered by entrapment.

Acknowledgements

The authors gratefully acknowledge financial support from the National Natural Science Foundation of China (No. 51174229) and South Graphite CO., LTD.

References

- ADAMCZYK Z., WERONKI P., 1999, *Application of the DLVO theory for particle deposition problems*, Advances in Colloid and Interface Science, 83(1-3), 137-226.
- BERGSTROM L., 1997, *Hamaker constants of inorganic materials*, Advances in Colloid and Interface Science, (70), 125-169.
- BLASKETT K.S., 1960, *Some effects of depressants in the flotation of a lead ore*, Proc. 5th Int. Mineral Processing Cong., 409-429.
- CROSSLEY P., 1999, *Graphite—High-tech supply sharpens up*, Industrial Minerals, (386), 31-47.
- DONG F.Z., 1997, *A study on flotation of a cryptocrystalline graphite ore*, Conservation and Utilization of Mineral Resources, (1), 15-17.

- CHIBOWSKI E., PEREA-CARPIO R., 2002, *Problems of contact angle and solid surface free energy determination*, Advances in Colloid and Interface Science, 98(2), 245-264.
- GAO H.M., YUAN J.Z., WANG X., GUAN J., ZHANG L., JING Z., MAO Y.L., 2007, *Mechanism of surface modification for sericite*, Journal of Wuhan University of Technology--Materials Science Edition, 22(3), 470-472.
- GEORGE P., NGUYEN A.V., JAMESON G.J., 2004, *Assessment of true flotation and entrainment in the flotation of submicron particles by fine bubbles*, Minerals Engineering, 17(7-8), 847-853.
- HE M., 2009, *The influence of adsorbed polymer on clay and copper mineral particles' interactions*, Doctoral Dissertation, Applied Science, University of South Australia, Brisbane, 2-3.
- JI G.C., 1991, *Continuous flotation experiment of microcrystalline graphite*, Non-metallic Mines, (2), 16-18.
- LI H.Q., FENG Q.M., YANG S.Y., OU L.M., LU Y., 2014, *The entrainment behaviour of sericite in microcrystalline graphite flotation*, International Journal of Mineral Processing, (127), 1-9.
- MITCHELL T.K., NGUYEN A.V., EVANS G.M., 2005, *Heterocoagulation of chalcopyrite and pyrite minerals in flotation separation*, Advances in Colloid and Interface Science, 114-115227-237.
- NGUYEN A.V., EVANS G.M., JAMESON G.J., 2002, *Approximate calculations of electrical double-layer interaction between spheres*. Encyclopedia of surface and colloid science. H. AT. New York, Marcel Dekker.
- MAURER S., MERSMANN A., PEUKERT W., 2001, *Henry coefficients of adsorption predicted from solid Hamaker constants*, Chemical Engineering Science, 56(11), 3443-3453.
- SALGADO M.R., 2001, *Upgrading the graphite by flotation at Bogala Mines in Sri Lanka*, J. Cent. South Univ. Technol., 8(3), 193-196.
- SILVESTER E., 2011, *The recovery of sericite in flotation concentrates*, Mineral Processing and Extractive Metallurgy, 120(1), 10-14.
- SIMANDL G.J., KENANL W.M., 1997, *Microcrystalline graphite*, British Columbia Geological Survey Geological Fieldwork, 240-241 240-244.
- WAN Q.H., 1997, *Effect of electrical double-layer overlap on the electroosmotic flow in packed-capillary columns*, Analytical Chemistry, 69(3), 361-363.
- WANG B., PENG Y., 2013, *The behaviour of mineral matter in fine coal flotation using saline water*, Fuel, 109309-315.
- WARREN L.J., 1985, *Determination of the contributions of true flotation and entrainment in batch flotation tests*, International Journal of Mineral Processing, 14(1), 33-44.
- XIA Y.K., REN Z.M., CHEN H.X., GUAN F.T., 1996, *A novel flotation flowsheet of microcrystalline graphite and its industrial application*, Non-metallic Mines, 19963.
- ZHENG X., JOHNSON N.W., FRANZIDIS J.P., 2006, *Modelling of entrainment in industrial flotation cells: Water recovery and degree of entrainment*, Minerals Engineering, 19(11), 1191-1203.